

EFFECTIVE IMAGE TAMPERING LOCALIZATION VIA ENHANCED TRANSFORMER AND CO-ATTENTION FUSION

Kun Guo^{1,2}, Haochen Zhu^{1,2}, Gang Cao^{1,2*}

¹State Key Laboratory of Media Convergence and Communication, Communication University of China, Beijing 100024, China

²School of Computer and Cyber Sciences, Communication University of China, Beijing 100024, China

ABSTRACT

Powerful manipulation techniques have made digital image forgeries be easily created and widespread without leaving visual anomalies. The blind localization of tampered regions becomes quite significant for image forensics. In this paper, we propose an effective image tampering localization network (EITLNet) based on a two-branch enhanced transformer encoder with attention-based feature fusion. Specifically, a feature enhancement module is designed to enhance the feature representation ability of the transformer encoder. The features extracted from RGB and noise streams are fused effectively by the coordinate attention-based fusion module at multiple scales. Extensive experimental results verify that the proposed scheme achieves the state-of-the-art generalization ability and robustness in various benchmark datasets. Code will be public at <https://github.com/multimediaFor/EITLNet>.

Index Terms— Image forensics, Tampering localization, Transformer, Coordinate attention

1. INTRODUCTION

Nowadays, digital image forgery has been drawing ever-increasing attention in our lives. As convenient editing tools are available, digital images can be tampered easily. Such tampered images are visually indistinguishable from original images and may lead to malicious use [1, 2]. Therefore, to fight against image forgery, it is crucial to accurately locate the tampered regions. Among many manipulation types, splicing, copy-move, and object removal are the three common semantic tampering techniques that have been studied most [3]. Splicing means to insert a region copied from a different image while copy-move refers to replicating an object from the same image. Removal, also known as inpainting, involves removing selected object region by extending the background. Such content-changed operations may cause serious misunderstandings. Generally, to better create realistic forgeries, some non-content-changed manipulations are also applied, such as brightness adjustment, Gaussian blur and JPEG compression. Since those manipulations do not

affect the semantic information expressed in the image scene, our study focuses on three main types of image manipulation techniques, splicing, copy-move, and removal.

Many deep learning-based approaches have been proposed for image forgery localization with different backbones. Noiseprint [4] leverages Siamese network to capture the imaging model-related artifacts. Zhou *et al.* [5] present a two-stream network that consists of RGB and noise residual branches based on Faster R-CNN. Full convolution networks are used to capture specific or generic forensic clues [1, 4, 6]. Furthermore, different attention modules are adopted to focus on tampered regions in a target image [2, 5, 7]. In MVSS-Net [2], dual attention strategy [8] is applied to feature fusion at the late stage. A forgery attention module is integrated to a coarse-to-fine network [5]. Liu *et al.* [7] exploits spatial-channel correlation attention mechanism in a progressive network.

Note that the prior methods often simply concatenate the RGB and noise view branches at an early or late stage for fusion, and ignore the interaction between two modalities. Additionally, attention modules are predominantly deployed in the decoder [7] or at a single scale [2], so they are not integrated well into the localization network. To attenuate such deficiency of existing works, we propose a new effective image tampering localization network (EITLNet) with high generalization performance and robustness. It leverages both high and low levels of operation trace features by an enhanced two-branch transformer network with co-attention feature fusion. A feature enhancement (FE) module is used to strengthen the feature representation ability of encoder. The coordinate attention-based fusion (CAF) module is designed to integrate the RGB and noise feature streams effectively across multiple scales. It promotes the interlacing and calibration of complementary information between the two branch sub-networks. Extensive evaluation results verify the superior accuracy of EITLNet on benchmark datasets and their online social network processing versions.

The remainder of the paper is organized as follows. In Section II, we present our proposed scheme in detail. Followed by extensive experimental results and discussions in Section III. We draw the conclusions in Section IV.

*Corresponding author

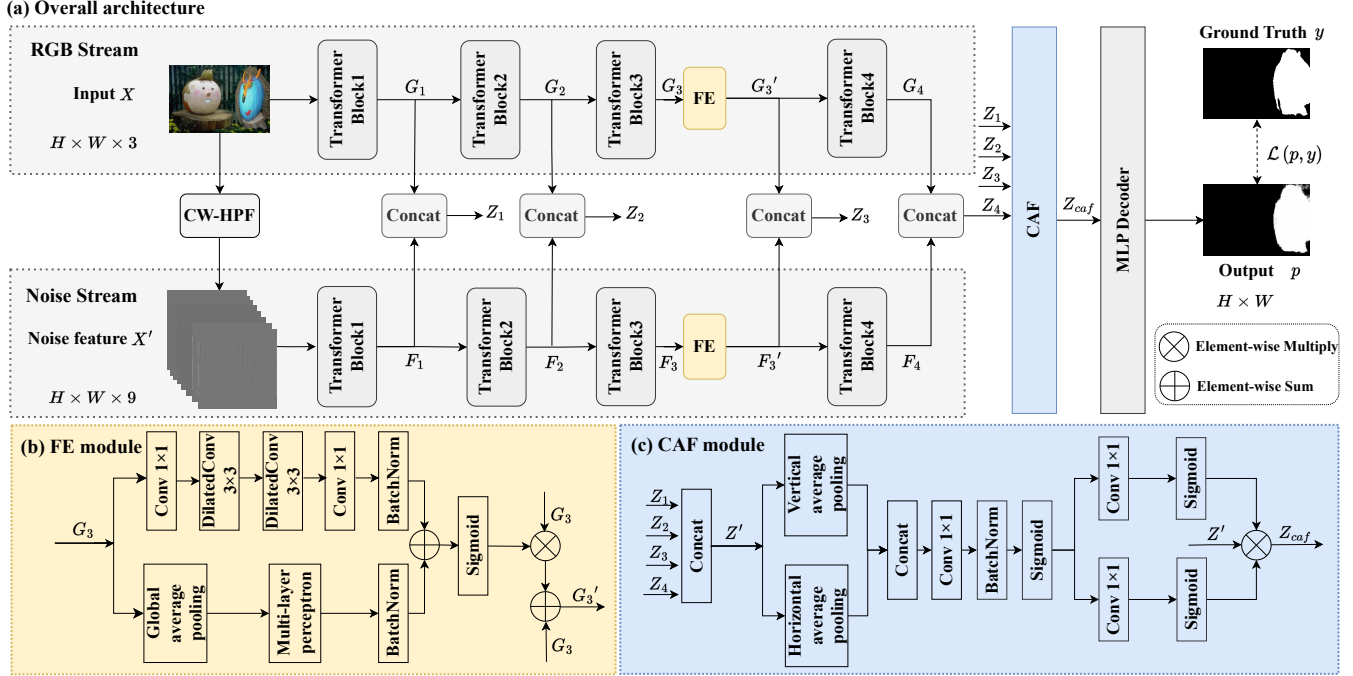


Fig. 1. Architecture of the proposed EITLNet.

2. PROPOSED SCHEME

2.1. Overview

Overview of the proposed tampering localization scheme is illustrated in Fig. 1. The Segformer [9] network is used as backbone. To capture forensic clues, the RGB and noise features are extracted by two branches, each with four transformer blocks and a FE module. The transformer blocks are based on the Mix Transformer encoder Mit-B2. Features at each scale are finally fused with a CAF module for enhancing the interaction between RGB and noise models. Meanwhile, we adopt a multilayer perceptron (MLP) as decoder, which consists of an upsampling layer and a linear layer. Additionally, channel-wise high pass filters (CW-HPF) [5] is used to extract noise with enlarged inter-channel inconsistency.

Specifically, we input an image X of size $H \times W \times 3$, as shown in Fig. 1., X passes through the CW-HPF block and outputs a noise feature map X' of size $H \times W \times 9$. X and X' are input to their corresponding feature-extraction branches. Then the feature maps at four levels are denoted as Z_n , ($n = 1, 2, 3, 4$) with resolutions of $1/4, 1/8, 1/16, 1/32$ of the original image respectively. We concatenate these four different scale feature maps correspondingly with a CAF module. Finally, the fused features are put into MLP decoder and predict a mask $P \in \mathbb{R}^{H \times W}$. The overview of our network is conceptually expressed as

$$P \leftarrow \text{MLP}(\text{CAF}(Z_1, Z_2, Z_3, Z_4)) \quad (1)$$

2.2. Feature enhanced module

To improve the feature representation ability of transformer encoders, an enhancement module is applied to the feature maps extracted by the middle transformer block. Such deployment is aimed at leveraging the high frequency features extracted from proper level of layers. As pointed out in [10], the features extracted from shallow transformer layers are so noisy that the performance may degraded. The features from deep layers have less high frequency information.

Detailed architecture of the feature enhancement module is in Fig. 1 (b). Given the feature map $G_3 \in \mathbb{R}^{H_3 \times W_3 \times C_3}$ yielded by the middle transformer block3 in RGB stream, the dilated convolutions $\text{conv}_{3 \times 3}^{\text{dila}}$ [11] are used to enlarge the receptive fields [12]. Two 1×1 convolutions $\text{conv}_{1 \times 1}$ are used to adjust the number of feature map channels. In detail, the spatial attention map $M_s(G_3)$ is generated as

$$M_s(G_3) = \text{BN}(\text{conv}_{1 \times 1}(\text{conv}_{3 \times 3}^{\text{dik}}(\text{conv}_{3 \times 3}^{\text{dik}}(\text{conv}_{1 \times 1}(G_3)))))) \quad (2)$$

where BN denotes batch normalization. Furthermore, the inter-channel relationship is leveraged to form the channel attention. To aggregate the feature map in each channel, global average pooling (GAP) is applied to G_3 and produce a $\mathbb{R}^{1 \times 1 \times C_3}$ channel feature map. Then MLP is adopted followed a batch normalization layer. That is,

$$M_c(G_3) = \text{BN}(\text{MLP}(\text{GAP}(G_3))) \quad (3)$$

Then we combine the $M_s(G_3)$ and $M_c(G_3)$ by element-wise

summation and take a sigmoid function to obtain the final attention map $M(G_3)$ as

$$M(G_3) = \text{sigmoid}(M_s(G_3) + M_c(G_3)) \quad (4)$$

Finally, the enhanced feature map G_3' is acquired as

$$G_3' = G_3 + G_3 \otimes M(G_3) \quad (5)$$

where \otimes denotes element-wise multiplication. The corresponding enhanced feature map F_3' is also yielded by applying the same module to the feature map F_3 of noise branch.

2.3. Coordinate attention-based fusion module

As illustrated in Fig. 1 (c), the features of two branches are first concatenated to be $Z' = [Z_1, Z_2, Z_3, Z_4]$. Then average pooling in horizontal and vertical directions are used to aggregate features respectively, as

$$Z'(h) = \text{HAP}(Z') \quad (6)$$

$$Z'(w) = \text{VAP}(Z') \quad (7)$$

where HAP is the horizontal average pooling and VAP is the vertical average pooling [13]. The spatial information is encoded horizontally and vertically as T in Eq. (8).

$$T = \text{sigmoid}(\text{BN}(\text{conv}_{1 \times 1}([Z'(w), Z'(h)]))) \quad (8)$$

where $[\cdot \cdot \cdot]$ denotes the concatenate operation. Then we split T along the spatial dimension to two separate tensors, T^h and T^w . Such are expanded and used as attention maps. The attention map M_h is yielded as

$$M_h = \text{sigmoid}(\text{conv}_{1 \times 1}(T^h)) \quad (9)$$

The M_w is yielded likewise. Finally, the fused feature Z_{caf} from CAF module is acquired as

$$Z_{caf} = Z' \otimes M_h \otimes M_w \quad (10)$$

2.4. Loss function

First, we employ the dice loss [14] used commonly in semantic segmentation networks is defined as

$$\mathcal{L}_{Dice}(p, y) = 1 - \frac{2 \sum p_i \cdot y_i}{\sum p_i^2 + \sum y_i^2} \quad (11)$$

where p_i and y_i are the prediction labels and ground truth for each pixel of the sample image respectively. Then, to address the issue of imbalanced positive and negative sample distribution. The focal loss [15] is defined as

$$\begin{aligned} \mathcal{L}_{Focal}(p, y) = & - \sum \alpha(1 - p_i)^\gamma y_i \log(p_i) \\ & - \sum (1 - \alpha)p_i^\gamma (1 - y_i) \log(1 - p_i) \end{aligned} \quad (12)$$

where the hyperparameters γ and α are the weights, for making the model focus on learning from more difficult samples.

Overall, the final loss function is defined as

$$\mathcal{L}(p, y) = \mathcal{L}_{Focal}(p, y) + \mathcal{L}_{Dice}(p, y) \quad (13)$$

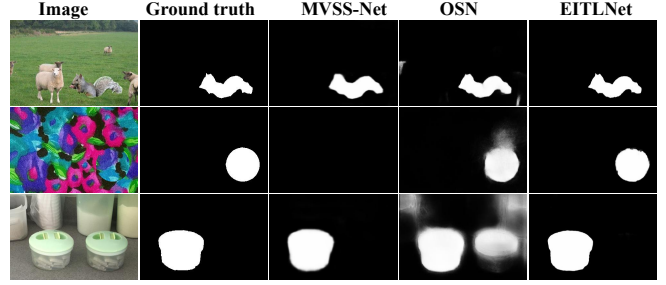


Fig. 2. Examples of localization results. From left to right: tampered images, ground truth, localization maps of the localizers including MVSS-Net, OSN and EITLNet.

3. EXPERIMENT

3.1. Experimental settings

Training Dataset. Following the prior work [16], a total of 60971 synthetic tampered images are used to train the proposed EITLNet. They are collected from a public synthetic image datasets [17] and CASIAv2 [18]. The synthetic forged images are created by splicing the pristine images with the object regions from MS-COCO [19].

Testing Dataset. Six commonly-used standard datasets are adopted for testing, including Coverage [20], CASIA-v1 [18], Columbia [21], NIST16 [22], DSO [23] and IMD [24].

Implementation Details. All images are resized to 512×512 pixels, and then enforced by general data augmentations including flip, scaling, Gaussian blur and JPEG compression. The network is initialized by the weights pretrained on ImageNet and trained for 100 epochs with the batch size 8 and a learning rate with cosine decay from $5e-3$ to $5e-4$. An AdamW optimizer is used with a momentum of 0.9. The related parameters are set empirically as $\alpha = 0.5$ and $\gamma = 2$.

3.2. Comparison with other localization algorithms

Performance of our proposed tampering localization scheme is compared with other state-of-the-art ones, which include Mantra-Net [1], DFCN [25], MVSS-Net [2], and OSN [6]. For fair comparison, the DFCN model is retrained on our training dataset. For other methods, we conducted tests using official publicly available code and models. Following the prior work [27], some NIST16 [22] images which can not be tested by ManTra-Net due to GPU memory limit are cropped to 2048×1440 pixels. Table 1 shows the localization results of different methods in terms of F1 and IoU [6]. Our method achieves the most superior average performance, outperforming the second-best method OSN by 6.2% and 9.0% in terms of F1 and IoU, respectively. It is observed that our proposed scheme always ranks the top two on each dataset, and consistently outperforms all the competing methods in terms of IoU. Fig. 2 provides a more intuitive insight into the actual

Table 1. Performance comparison of different tampering localization algorithms on different datasets (F1 and IoU). The best results of per test sets are highlighted in bold font. “-” indicates not applicable.

Methods	Columbia		CASIA-v1		DSO		NIST		Coverage		IMD		Average	
	F1	IoU	F1	IoU	F1	IoU	F1	IoU	F1	IoU	F1	IoU	F1	IoU
Mantra-Net, CVPR19 [1]	0.357	0.258	0.130	0.086	0.332	0.243	0.088	0.054	0.275	0.186	0.183	0.124	0.228	0.159
Noiseprint, TIFS20 [4]	0.364	0.262	-	-	0.339	0.253	0.122	0.081	0.147	0.087	0.179	0.120	0.230	0.161
DFCN, TIFS21 [25]	0.419	0.280	0.181	0.119	0.320	0.217	0.082	0.055	0.263	0.157	0.233	0.161	0.250	0.165
MVSS-Net, ICCV21 [26]	0.684	0.596	0.451	0.397	0.271	0.188	0.294	0.240	0.445	0.379	0.260	0.200	0.401	0.333
OSN, TIFS22 [6]	0.707	0.608	0.509	0.465	0.436	0.308	0.332	0.255	0.260	0.176	0.491	0.392	0.456	0.367
EITLNet	0.881	0.851	0.530	0.492	0.410	0.319	0.308	0.256	0.448	0.371	0.532	0.455	0.518	0.457

Table 2. Ablation analysis of our proposed scheme (F1 and IoU). The best results of per test sets are highlighted in bold font.

Methods	Columbia		CASIA-v1		DSO		NIST16		Coverage		IMD		Average	
	F1	IoU	F1	IoU	F1	IoU	F1	IoU	F1	IoU	F1	IoU	F1	IoU
Baseline	0.828	0.782	0.533	0.498	0.368	0.284	0.273	0.225	0.351	0.276	0.530	0.455	0.480	0.420
Baseline+CAF	0.861	0.827	0.547	0.508	0.380	0.295	0.302	0.249	0.445	0.360	0.525	0.449	0.510	0.448
Baseline+CAF+FE	0.881	0.851	0.530	0.492	0.410	0.319	0.308	0.256	0.448	0.371	0.532	0.455	0.518	0.457

Table 3. Robustness evaluation results against the social media networks (F1). The datasets are uploaded on Facebook(Fb), Weibo(Wb), WeChat(Wc), WhatsApp(Wa).

Methods	Columbia				CASIA-v1				DSO				NIST16				Average			
	Fb	Wb	Wc	Wa	Fb	Wb	Wc	Wa	Fb	Wb	Wc	Wa	Fb	Wb	Wc	Wa	Fb	Wb	Wc	Wa
DFCN	0.315	0.172	0.404	0.306	0.161	0.159	0.196	0.174	0.049	0.056	0.167	0.225	0.116	0.075	0.005	0.183	0.160	0.115	0.204	0.222
MVSS-Net	0.691	0.689	0.690	0.685	0.387	0.403	0.248	0.359	0.277	0.258	0.214	0.181	0.264	0.251	0.212	0.165	0.405	0.400	0.341	0.348
OSN	0.714	0.724	0.727	0.727	0.462	0.466	0.405	0.478	0.447	0.370	0.366	0.341	0.329	0.294	0.286	0.313	0.488	0.464	0.446	0.465
EITLNet	0.803	0.896	0.890	0.911	0.473	0.453	0.364	0.490	0.312	0.354	0.363	0.396	0.370	0.343	0.327	0.349	0.489	0.511	0.486	0.536

quality of the results by visualizing examples.

3.3. Ablation study

In order to assess the individual impact of the main design choices of our approach, we conduct several ablative experiments. All of these experiments are carried out on the same datasets for training. The baseline model contains a network with RGB and CW-HPF noise stream and concatenate modules, without FE and CAF modules. Table 2 indicates that adopting CAF leads to an average increase of 3.0 % in the F1 score compared to simple concatenation, along with a 2.8 % improvement in IoU score. Such results prove the efficiency of our proposed fusion module. The last row of Table 2 illustrates the effect of the FE module. The performance increases to 51.8 % in F1 and 45.7 % in IoU on average, which verifies the advantages of the FE module.

3.4. Robustness evaluation

As various lossy operations on social networks pose significant challenges to the robustness of image tampering localization [6], we evaluate the robustness of our model against the postprocessing to the social media platforms.

Specificly, the dataset proposed in OSN are evaluated. The four standard forensic datasets are uploaded on Facebook, Weibo, WeChat, and WhatsApp. As illustrated in Table 3, our method shows a consistent gain over all social platforms on Columbia and NIST16 dataset, and achieves competitive performances against the social media networks with other tested platforms. On average, the F1 score has increased on average by 4.7%, 4%, 7.1% on Weibo, WeChat, WhatsApp.

4. CONCLUSION

In this paper, we proposed a novel image tampering localization scheme that leverages a two-branch enhanced transformer encoder and co-attention feature fusion. The feature enhancement module is utilized to strengthen the network representation and the coordinate attention-based fusion module is adopt to combine the multi-scales features. Extensive experiments show that our proposed method achieves superior performance than state-of-the-art models. The EITLNet is verified to be robust against the different social media platforms. In future work, we aim to explore the extension of the proposed method to incorporate noise-based fusion with other approaches.

5. REFERENCES

- [1] Yue Wu, Wael AbdAlmageed, and Premkumar Natarajan, “Mantra-net: Manipulation tracing network for detection and localization of image forgeries with anomalous features,” in *Computer Vision and Pattern Recognition*, 2019, pp. 9543–9552.
- [2] Chengbo Dong, Xinru Chen, Ruohan Hu, Juan Cao, and Xirong Li, “Mvss-net: Multi-view multi-scale supervised networks for image manipulation detection,” *IEEE Transactions on Pattern Analysis and Machine Intelligence*, vol. 45, no. 3, pp. 3539–3553, 2022.
- [3] N.Memon H.T.Sencar, L.Verdoliva, “Multimedia forensics,” *Computer Vision and Pattern Recognition*, pp. 281–284, 2022.
- [4] Davide Cozzolino and Luisa Verdoliva, “Noiseprint: A cnn-based camera model fingerprint,” *IEEE Transactions on Information Forensics and Security*, vol. 15, pp. 144–159, 2019.
- [5] Long Zhuo, Shunquan Tan, Bin Li, and Jiwu Huang, “Self-adversarial training incorporating forgery attention for image forgery localization,” *IEEE Transactions on Information Forensics and Security*, vol. 17, pp. 819–834, 2022.
- [6] Haiwei Wu, Jiantao Zhou, Jinyu Tian, Jun Liu, and Yu Qiao, “Robust image forgery detection against transmission over online social networks,” *IEEE Transactions on Information Forensics and Security*, vol. 17, pp. 443–456, 2022.
- [7] Xiaohong Liu, Yaojie Liu, Jun Chen, and Xiaoming Liu, “Psc-net: Progressive spatio-channel correlation network for image manipulation detection and localization,” *IEEE Transactions on Circuits and Systems for Video Technology*, vol. 32, no. 11, pp. 7505–7517, 2022.
- [8] Jun Fu, Jing Liu, Haijie Tian, Yong Li, Yongjun Bao, Zhiwei Fang, and Hanqing Lu, “Dual attention network for scene segmentation,” in *Computer Vision and Pattern Recognition*, 2019, pp. 3146–3154.
- [9] Enze Xie, Wenhai Wang, Zhiding Yu, Anima Anandkumar, Jose M Alvarez, and Ping Luo, “Segformer: Simple and efficient design for semantic segmentation with transformers,” in *Neural Information Processing Systems*, 2021.
- [10] Chao Yang, Zhiyu Wang, Huawei Shen, Huizhou Li, and Bin Jiang, “Multi-modality image manipulation detection,” in *International Conference on Multimedia and Expo*, 2021.
- [11] Fisher Yu and Vladlen Koltun, “Multi-scale context aggregation by dilated convolutions,” in *International Conference on Learning Representations*, 2016.
- [12] Jongchan Park, Sanghyun Woo, Joon-Young Lee, and In So Kweon, “Bam: Bottleneck attention module,” *arXiv preprint arXiv:1807.06514*, 2018.
- [13] Qibin Hou, Daquan Zhou, and Jiashi Feng, “Coordinate attention for efficient mobile network design,” in *Computer Vision and Pattern Recognition*, 2021, pp. 13713–13722.
- [14] Qijie Wei, Xirong Li, Weihong Yu, Xiao Zhang, Yongpeng Zhang, Bojie Hu, Bin Mo, Di Gong, Ning Chen, Dayong Ding, et al., “Learn to segment retinal lesions and beyond,” in *International Conference on Pattern Recognition*, 2021, pp. 7403–7410.
- [15] Tsung-Yi Lin, Priya Goyal, Ross Girshick, Kaiming He, and Piotr Dollár, “Focal loss for dense object detection,” in *International Conference on Computer Vision*, 2017, pp. 2980–2988.
- [16] Haochen Zhu, Gang Cao, and Mo Zhao, “Effective image tampering localization with multi-scale convnext feature fusion,” *arXiv preprint arXiv:2208.13739*, 2022.
- [17] Jawadul H Bappy, Amit K Roy-Chowdhury, Jason Bunk, Lakshmanan Nataraj, and BS Manjunath, “Exploiting spatial structure for localizing manipulated image regions,” in *International Conference on Computer Vision*, 2017, pp. 4970–4979.
- [18] Jing Dong, Wei Wang, and Tieniu Tan, “Casia image tampering detection evaluation database,” in *China Summit and International Conference on Signal and Information Processing*, 2013, pp. 422–426.
- [19] Tsung-Yi Lin, Michael Maire, Serge Belongie, James Hays, Pietro Perona, Deva Ramanan, Piotr Dollár, and C Lawrence Zitnick, “Microsoft coco: Common objects in context,” in *European Conference on Computer Vision*, 2014, pp. 740–755.
- [20] Bihan Wen, Ye Zhu, Ramanathan Subramanian, Tian-Tsong Ng, Xuanjing Shen, and Stefan Winkler, “Coverage—a novel database for copy-move forgery detection,” in *International Conference on Image Processing*, 2016, pp. 161–165.
- [21] Yu-Feng Hsu and Shih-Fu Chang, “Detecting image splicing using geometry invariants and camera characteristics consistency,” in *International Conference on Multimedia and Expo*, 2006, pp. 549–552.
- [22] Haiying Guan, Mark Kozak, Eric Robertson, Yooyoung Lee, Amy N Yates, Andrew Delgado, Daniel Zhou, Timothee Kheyrkhan, Jeff Smith, and Jonathan Fiscus, “Mfc datasets: Large-scale benchmark datasets for media forensic challenge evaluation,” in *Winter Applications of Computer Vision Workshops*, 2019, pp. 63–72.
- [23] Tiago José De Carvalho, Christian Riess, Elli Angelopoulou, Helio Pedrini, and Anderson de Rezende Rocha, “Exposing digital image forgeries by illumination color classification,” *IEEE Transactions on Information Forensics and Security*, vol. 8, no. 7, pp. 1182–1194, 2013.
- [24] Adam Novozamsky, Babak Mahdian, and Stanislav Saic, “Imd2020: A large-scale annotated dataset tailored for detecting manipulated images,” in *Winter Conference on Applications of Computer Vision Workshops*, 2020, pp. 71–80.
- [25] Peiyu Zhuang, Haodong Li, Shunquan Tan, Bin Li, and Jiwu Huang, “Image tampering localization using a dense fully convolutional network,” *IEEE Transactions on Information Forensics and Security*, vol. 16, pp. 2986–2999, 2021.
- [26] Xinru Chen, Chengbo Dong, Jiaqi Ji, Juan Cao, and Xirong Li, “Image manipulation detection by multi-view multi-scale supervision,” in *International Conference on Computer Vision*, 2021, pp. 14185–14193.
- [27] Myung-Joon Kwon, Seung-Hun Nam, In-Jae Yu, Heung-Kyu Lee, and Changick Kim, “Learning jpeg compression artifacts for image manipulation detection and localization,” *International Journal of Computer Vision*, vol. 130, no. 8, pp. 1875–1895, 2022.